Hindawi
Journal of Sensors
Volume 2021, Article ID 8819402, 13 pages
https://doi.org/10.1155/2021/8819402

Research Article

Detecting Electromagnetic Geographical Environment Changes Based on the Frequency-Intensity Curve

Yi Huang[1,2,3] **Mengyi Wang**,[4] **Qianqian Qiu**,[5] **Lizhi Miao**,[2,3] **Haiping Zhang**,[1,6] **Jiarui Qin**,[1,6] **Xiangqiang Min**,[1,6] **and Yehua Sheng**[1,6]

[1]*Key Laboratory of Virtual Geographic Environment (Nanjing Normal University), Ministry of Education, 210023, China*
[2]*School of Geographic and Biologic Information, Nanjing University of Posts and Telecommunications, 210023, China*
[3]*Smart Health Big Data Analysis and Location Services Engineering Lab of Jiangsu Province, Nanjing University of Posts and Telecommunications, 210023, China*
[4]*Zhejiang Wenling High School, 317515, China*
[5]*Jiangsu Province Surveying & Mapping Engineering Institute, China*
[6]*Jiangsu Center for Collaborative Innovation in Geographical Information Resource Development and Application, Nanjing Normal University, 210023, China*

Correspondence should be addressed to Yehua Sheng; shengyehua@njnu.edu.cn

Received 8 September 2020; Revised 28 September 2021; Accepted 22 October 2021; Published 16 November 2021

Academic Editor: Manel Gasulla

Electromagnetic geographic environment is closely related to human life. With continuous popularization of public infrastructures and daily electronic instruments, such as electric power communication systems and household appliances, electromagnetic radiation sources have increased sharply in the geographic environment, which leads to increasingly serious electromagnetic radiation pollution. Thus, it is significant to monitor, evaluate, and analyze the electromagnetic radiation condition and explore its changing law in the environment. However, the traditional monitoring method can only detect anomalies within certain frequencies in the fixed stations. To fill this gap, this research first develops a vehicle-mounted electromagnetic environment monitoring system to collect both spatial positioning data and electromagnetic data of the whole frequency range. The acquired data are then used to construct the location-based frequency-intensity curve to reflect the variation of electromagnetic radiation at different frequency ranges. On this basis, a curve similarity measurement method is introduced to analyze the similarity of different curves, which is effective to diagnose time-varying sources from both global and local perspectives. This research provides a real-time mobile monitoring method, which is significant to know the dynamic variation of local electromagnetic environment and promotes subsequent comprehensive geographic analyses.

1. Introduction

Electromagnetic environment is an external manifestation of electromagnetic space, which refers to the sum of all electromagnetic phenomena existing in a certain time, space, and frequency [1–3]. The geographic environment where people live in is filled by an imperceptible electromagnetic field and can be seen as an electromagnetic geographical environment with a characteristic of time-space-frequency [4]. With the widespread application of public infrastructures (power communication systems, domestic appliances, electronic facilities, etc.), massive electromagnetic radiation sources increase environmental pollution and cause serious impacts on people's health [5, 6]. Therefore, it is significant to monitor, evaluate, and analyze the electromagnetic geographical environment scientifically and explore the variation rules of electromagnetic radiation in the geographical environment.

Electromagnetic environment monitoring is aimed at detecting the electromagnetic radiation intensity and distribution characteristics of the environment [7, 8]. In the 1940s, the harmfulness of electromagnetic radiation to aircraft and ancillary electronic equipment is first noticed by the U.S. military [9]. To control the electromagnetic interference of mechanical-electronic equipment, they formulate the

world's earliest specification for military electromagnetic interference (JAN-I-225). Afterwards, different high-power radio devices have been widely used in both military and civilian fields [10–12]. They can produce large amounts of electromagnetic radiation and restrict people's life. To reduce electromagnetic hazards, many researchers have conducted in-depth studies in this field. For instance, electromagnetic environment criteria are proposed to regulate the application of electromagnetic equipment [13]. Different kinds of radio monitoring software are developed to detect the electromagnetic environmental condition and analyze the electromagnetic spectrum [14–16]. Through continuous improvement of the monitoring and management system, studies on electromagnetic environment monitoring have become more mature and reasonable. Many developed countries have established relatively perfect databases and realized the remote automatic monitoring and management system of electromagnetic environment [17].

During the process of signal acquisition, conversion, and transmission, electromagnetic data are often affected by equipment, environment, or other factors and can be inevitably contaminated by different types of noise [18, 19]. To eliminate errors induced by these noises, data preprocessing of measured signals is necessary for the subsequent diagnosis and analysis. Smoothing, also known as a digital filter, is one of the most prevalent preprocessing methods. There are various filtering methods, such as mean filtering, median filtering, Gaussian filtering, and exponential filtering [20–23]. Different methods have distinct advantages and disadvantages in dealing with different types of noise. Thus, it is necessary to select an appropriate filtering method according to the actual situation.

To diagnose anomalous changes in the electromagnetic environment, it is effective to construct the frequency-intensity curve of electromagnetic data and then compare their similarities based on distance measuring equations. Based on the types of distance, similarity measuring methods can be divided into three kinds (Euclidean distance-based, Hausdorff distance-based, and Fréchet distance-based). Among them, the Euclidean distance-based method does not fully consider every feature point and is not sensitive to the position of the feature band. In addition, curves are usually transformed (e.g., stretching and translation) when calculating the distance; it has obvious drawbacks to measure those curves which have shifted significantly [24]. The Hausdorff distance-based method is widely used to measure the similarity of two point sets and can solve the problem of image degradation, occlusion, and false intersection points [25]. However, this method focuses on points but not curves; it is hard to measure the similarity of curves as a whole [26]. In comparison, the Fréchet distance-based method considers the shape and continuity of the curve and sequence of each point. It is better at measuring curve similarity than the previous method and has been applied in various fields [27, 28].

To sum up, although electromagnetic environment monitoring has made considerable progress, there are still some deficiencies in the dynamic monitoring scheme and spatial analysis. From the perspective of the dynamic monitoring scheme, traditional methods mainly focus on a single radiation source (e.g., communication base station, traffic facilities, and high-voltage wire) and acquire monitoring data in fixed stations. Nevertheless, the variation of electromagnetic radiation is different in different locations and frequency bands. Monitoring in fixed stations cannot provide the variation data in a large area. Meanwhile, the conventional approach can only detect the electromagnetic signal within a narrow frequency range but not the whole frequency range. It is insufficient to monitor the complicated electromagnetic environment and unable to reliably evaluate the electromagnetic radiation condition of the entire region. From the perspective of spatial analysis, limited studies are conducted on the spatial variation regularities of the electromagnetic environment. Thus, it is urgently needed to establish an automatic method to diagnose spatial variation by mobile measurement, which is the primary step for detecting changing electromagnetic phenomena and their corresponding frequency bands, searching unknown radiation sources.

To overcome these deficiencies, this research first breaks through the limitation of the traditional electromagnetic monitoring method and develops a vehicle-mounted electromagnetic environment monitoring system (VEEMS) to collect the electromagnetic data of the whole frequency range. Based on the collected data, the electromagnetic frequency-intensity curve is constructed by integrating ideas from the ground object spectrum. Moreover, the similarity of electromagnetic frequency-intensity curves of adjacent sampling points is analyzed to detect anomalous changes in different locations and bands. It provides clues for searching potential radiation sources, improves the scientific management level of electromagnetic geographical environment, and lays a foundation for further environmental analysis and evaluation. It should be noted that the anomalous changes in this research refer to the changing power level of electromagnetic signals which exceed a preset threshold.

The rest of this paper is organized as follows. We develop VEEMS and make explicit the data organization and management methods in the second section. We integrate the concept of the ground object spectrum and propose a detection method in the third section. The local changing sources are then detected and analyzed in the fourth section from both local and global perspectives. Finally, the conclusions and future works are discussed in the last section.

2. Development of VEEMS and Data Organization

2.1. Development of VEEMS. Since the electromagnetic radiation condition is complicated in the urban area, a mobile monitoring system which can detect a broad frequency range is needed. Such system should integrate multiple detectors for different frequencies and work synchronously to measure the data. In addition, the system needs to install a spatial positioning device taking account of the spatial variation of electromagnetic environment. Thus, we develop the VEEMS (Figure 1) which integrates the GNSS (Global Navigation Satellite System) positioning device, electromagnetic radiation detectors (six spectrometers and four

(a) Exterior of the system (b) Interior of the system

Figure 1: The appearance of VEEMS.

electromagnetic probes), wide bandwidth antenna, signal amplification and transformation devices, controller, etc. It is a real-time synchronous acquisition system which can collect both electromagnetic radiation data and location data.

Specifically, VEEMS adopts both selective frequency and nonselective frequency methods to detect radiation field intensity. The electromagnetic detectors collect data every 10 seconds, while each device is responsible for acquiring different frequencies in X, Y, Z directions (note: three directions where the antennas are pointing to). The data from different directions are then combined by Equations (1) and (2) to calculate synthetic intensities of the electromagnetic probe (DTT) and spectrometer (PPY), respectively:

$$\text{sumIntensity\_DTT} = \sqrt{\text{Intensity}X^2 + \text{Intensity}Y^2 + \text{Intensity}Z^2}, \quad (1)$$

$$\text{sumIntensity\_PPY} = \frac{(\text{Intensity}X + \text{Intensity}Y + \text{Intensity}Z)}{3}. \quad (2)$$

According to the actual situation, parameters of the system (e.g., data type, frequency, number of frequency point, and step size) are set in Table 1. Additionally, the GNSS device collects positioning data per second.

2.2. Data Organization and Management. VEEMS integrates multiple devices to collect electromagnetic data and positioning data automatically and then saves these data as several files in the storage according to the type of detectors, such as GNSS data file, PPY data file, and DTT data file. Among them, the GNSS data file records the trajectory information of VEMMS, including GGA (GPS Fix Data), GSA (GPS DOP and Active Satellites), GSV (GPS Satellites in View), RMC (Recommended Minimum Specific), and VTG (Track Made Good and Ground Speed). These records save rich information such as time, latitude, longitude, and magnetic declination. The PPY data file also records abundant information, which is data acquisition time, IP of each spectrometer, ID of each detector, resolution bandwidth, starting frequency, ending frequency, time interval, and high-frequency electric field power.

Compared with GNSS and PPY files, DDT data can be further divided into two kinds based on the types of detector. First, detectors marked as ID 7, 8 can obtain both electric and magnetic data. The collected data include time, ID, starting frequency, ending frequency, step size, filter bandwidth, data type, direction, and the intensity of the electromagnetic field. The rest of two detectors (ID 9, 10) can only collect one type of data (electric field intensity or magnetic field intensity), but their contents are similar, in which each record includes time, ID, highest detecting frequency, data type, step size, filter bandwidth, and intensity at three directions (X/Y/Z).

The collected raw data should be further processed and stored in the database. Thus, we develop a corresponding program to finish this task. To be specific, GNSS data are converted into shapefile (point data) and stored in MDB (Microsoft Database); electromagnetic data are processed separately, and the generated text files are stored in SQL Server. Furthermore, to enrich the electromagnetic data with positioning information and construct a unified electromagnetic geographic database, we link two databases with reference to their collection time. Detailed procedures for data collection and processing can be seen in Figure 2.

3. Construction of Electromagnetic Anomaly Detection Method

The idea of electromagnetic radiation anomaly detection is shown in Figure 3, and the specific steps can be explained as follows: (1) construct electromagnetic frequency-intensity curves of each sampling point, and remove noises by accumulative curves and digital filters; (2) measure the similarity of constructed curves by utilizing Fréchet distance; and (3) conduct anomaly detections in both global and local perspectives based on the similarity measuring results.

3.1. Construction and Processing of Location-Based Frequency-Intensity Curve. VEEMS collects electromagnetic

Table 1: Parameters of different detectors.

Type	Detector	Frequency	Data type	Number of point	Step size
DTT	ID 9	0~100 kHz	Electric field	413 in $X/Y/Z$ direction	242.72 Hz
	ID 10	0~100 kHz	Magnetic field	413 in $X/Y/Z$ direction	242.72 Hz
	ID 7, ID 8	100 kHz~200 kHz	Electric & magnetic field	34	3030.30 Hz
PPY	ID 4~6	200 kHz~10 MHz	High-frequency electric field	461	21304.35 Hz
	ID 1~3	10 MHz~2 GHz[1]		461	4326086.96 Hz

[1]Although the upper limit of this detector reaches 12 GHz, we set the limit to 2 GHz, since the actual radiation frequency in this region does not exceed this value normally.

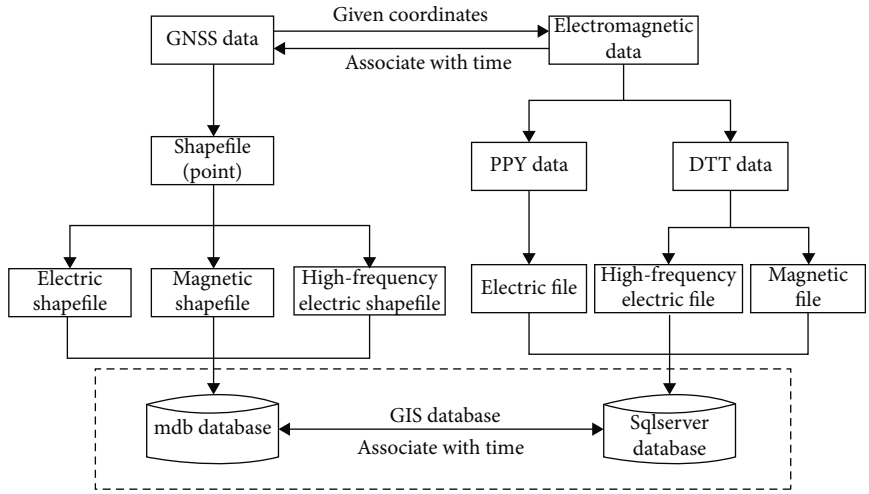

Figure 2: Data collection and processing.

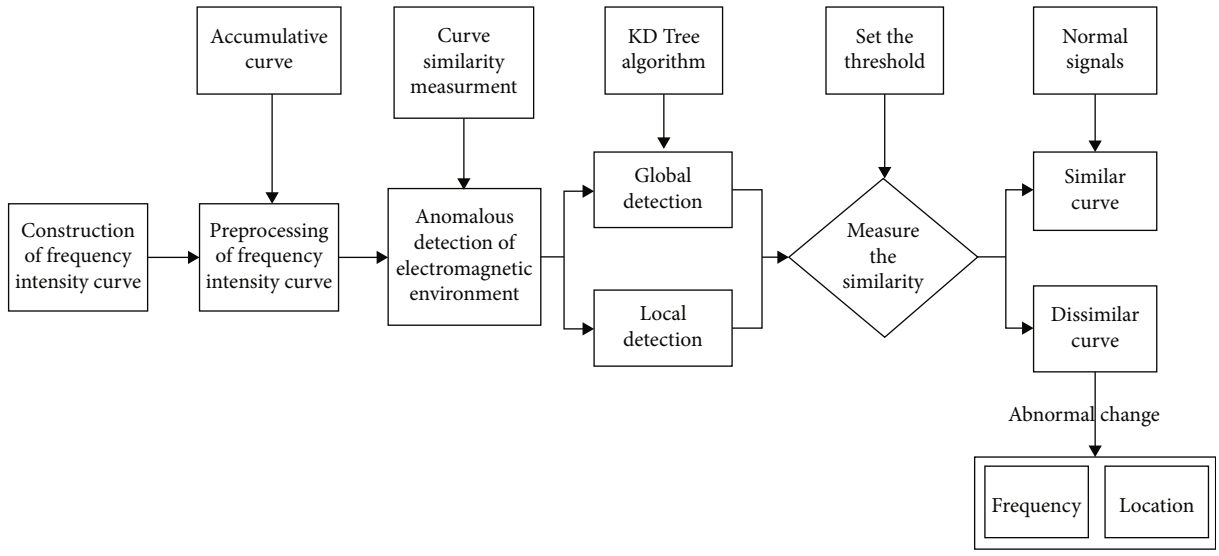

Figure 3: Basic steps for electromagnetic radiation anomaly detection.

intensity data effectively at different frequency ranges. To detect anomalous signals from these data, an effective analyzing method is needed. Thus, we integrate ideas from the ground object spectrum [29] and construct the frequency-intensity curve (Figure 4 as an example) to represent the electromagnetic radiation condition at different sampling points. Such a method lays a foundation for future anomaly detection of the electromagnetic environment.

After constructing the frequency-intensity curve, we have to recognize that the external environment as well as data acquisition devices may produce noises to disturb electromagnetic signals; therefore, the generated curves should

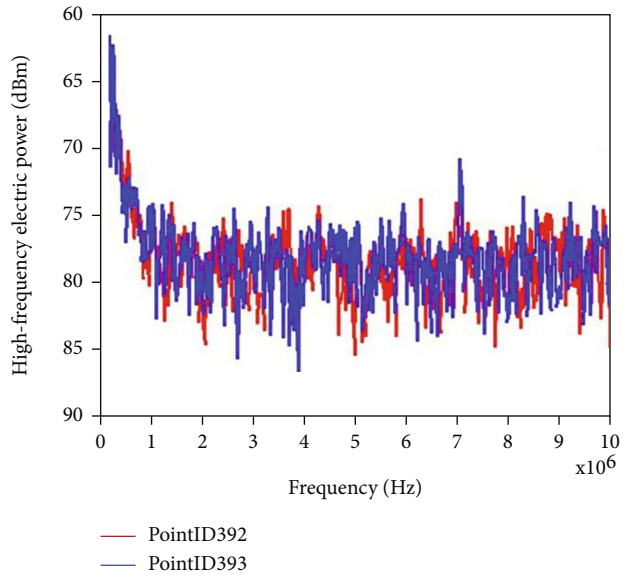

FIGURE 4: Frequency-intensity curves for the high-frequency electric field (200 K~10 M).

remove burrs caused by these noises and ensure the accuracy and reliability of the result. Therefore, we apply two methods (accumulative curve and digital filter) to preprocess the data, which can improve the Signal to Noise Ratio (SNR) and smooth the frequency-intensity curves.

The frequency-intensity accumulative curve accumulates electromagnetic intensity at different frequencies. It can remove random noises as a filter and display the variation trend intuitively. To be specific, the accumulative curve (S) selects frequency (x_i) as the horizontal axis and accumulative intensity (y_i^{acc}) as the vertical axis, which can be presented as

$$S = <(x_1, y_1^{\text{acc}}), (x_2, y_2^{\text{acc}}), \cdots, (x_i, y_i^{\text{acc}}), \cdots, (x_n, y_n^{\text{acc}}) > . \quad (3)$$

The accumulative intensity (y_i^{acc}) is calculated by the measured electromagnetic intensity (y_i) as

$$y_i^{\text{acc}} = \sum_{i=1}^{N} y_i. \quad (4)$$

Although the accumulative curve can remove some noises effectively, it is not suitable for all frequency ranges. Thus, a digital filter is needed in this study. We compare the results of four common filters, which are Gaussian filter, mean filter, median filter, and adaptive median filter. Since there are multiple frequencies and limited space, we just select one sampling point (ID 392) and the high-frequency electric field (200 kHz~10 MHz) as the example to show the results. In particular, the window size of the Gaussian filter (the square deviation, σ, is set as 0.3), mean filter, and median filter is 1×7, and the window size of adaptive median filter varies from 1×3 to 1×7. The results can be seen in Figure 5.

From Figure 5, the adaptive median filtering method proves to be the most effective approach to remove noises for some frequency ranges. It can reserve detailed characteristics and adjust the filter window adaptively according to the levels of noise pollution.

Eventually, the frequency-intensity accumulative curve is used for the frequency range as 0~100 kHz, and the adaptive median filtering method is applied for the rest of the three frequency ranges.

4. Electromagnetic Radiation Anomaly Detection Based on Curve Similarity Measurement

4.1. Algorithm for Curve Similarity Measurement. After constructing frequency-intensity curves, the curve similarity of different sampling points should be measured to identify anomalous changes. According to the previous discussion, we propose a measuring algorithm based on the discrete Fréchet distance [30]. To better understand the algorithm, we will first briefly elaborate on how the discrete Fréchet distance is calculated as follows.

Suppose two curves, A and B, are consisting of multiple discrete points as $A = <a_1, a_2, \cdots, a_m>$, $B = <b_1, b_2, \cdots, b_n>$, and these points can form a series of point sequences, that is, $W = \{(A_i, B_i)\}\ (1 \le i \le k)$, which consists of k coupling sequence as $(a_{u1}, b_{v1}), (a_{u2}, b_{v2}), \cdots, (a_{uk}, b_{vk})$, where $u_1 = 1$, $v_1 = 1$, $u_k = n$, $v_k = m$. Thus, the discrete Fréchet distance between curve A and B can be calculated by

$$d_F(A, B) = \min \max_{(a,b) \in A_i \times B_i} \text{dist}(a, b). \quad (5)$$

Based on the discrete Fréchet distance, we propose the corresponding algorithm, which can be explained as follows:

(1) Given two frequency-intensity curves A and B of m and n discrete points, respectively, that is, $A = <a_1, a_2, \cdots, a_m>$, $B = <b_1, b_2, \cdots, b_n>$, assuming $m \le n$

(2) Let curve A be the benchmark, and make Fréchet alignment for curve B. Then, curve B is divided into m arcs. Suppose k partitions meet the requirements and can be defined as

$$W_j = \{(A_i, B_i)\}\ (1 \le i \le m, 1 \le j \le k) \quad (6)$$

(3) For each $W_j = \{(A_i, B_i)\}$, calculate the largest distance from A_i to every point in B_i, that is, $d = |a_i -$

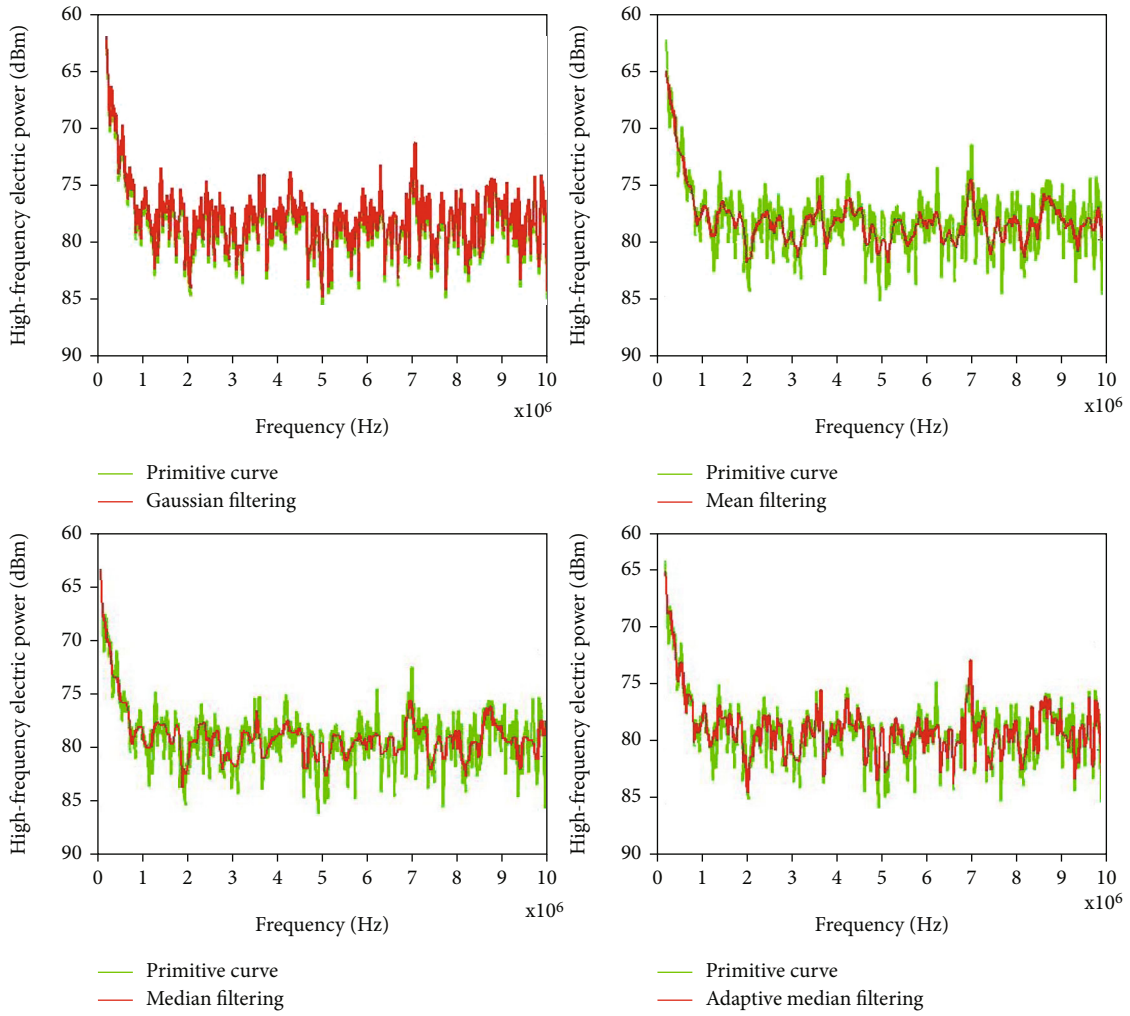

Figure 5: Results of different filters.

$b_j \mid (1 \le i \le m, 1 \le j \le n)$. Sort every d and get the maximum value from all largest distances as

$$d_F^W(A, B) = \max_i \max_{(a,b)\in A_i \times B_i} \operatorname{dist}(a, b) \tag{7}$$

(4) Find the smallest value from $d_F^W(A, B)$ as the optimal result. This value is the discrete Fréchet distance between curves A and B, which can be defined as

$$d_F(A, B) = \min_w d_F^W(A, B) \tag{8}$$

4.2. Local Detection for Anomalous Changes in Electromagnetic Geographic Environment. The above curve similarity measurement based on discrete Fréchet distance can detect anomalous changes in the electromagnetic geographic environment. To study the electromagnetic variation more effectively and comprehensively, we adopt both local and global detecting methods to analyze anomalous changes. The local detection method first extracts previous and later surrounding points of the current sampling point and then measures the similarity of frequency-intensity curves between these points. The basic principle of this method is to explore anomalous changes and their corresponding frequencies by comparing the similarity and given threshold. The threshold can be calculated by the following method.

Assuming the discrete Fréchet distance of the current sampling point is dF_i, and the discrete Fréchet distance of surrounding points is dF_j ($n = 2$, from dF_{i-n} to dF_{i+n}, except dF_i), then the threshold ε_i is the average value of dF_j, which can be defined as

$$\varepsilon_i = \frac{\sum_{j=i-n}^{i-1} dF_j}{n} \ (i \ge 4). \tag{9}$$

If $dF_i > \varepsilon_i$, the corresponding sampling point is judged as an anomalous point where unusual changes occurred in this

Table 2: Threshold of each frequency band.

Frequency (Hz)	Electric field		Magnetic field		High-frequency electric field	
	0~100 K	100 K~200 K	0~100 K	100 K~200 K	200 K~10 M	10 M-2 G
Threshold (ε_{max})	0.9880	3.2313	0.1994	0.1261	9.3791	6.6981

Table 3: Discrete Fréchet distances of ID 393 and its adjacent points.

Frequency (Hz)	Electric field		Magnetic field		High-frequency electric field	
	0~100 K	100 K~200 K	0~100 K	100 K~200 K	200 K~10 M	10 M-2 G
ID 390	7.3011	4.6118	3.2395	0.0381	9.3435	5.1323
ID 391	8.5636	3.4322	2.3834	0.0311	7.0051	5.0479
ID 392	2.4011	5.5605	2.3831	0.0928	8.2681	4.5961
ID393	2.6312	4.3504	0.4783	0.0238	7.4138	5.5456

Table 4: Threshold of ID 393.

Frequency (Hz)	Electric field		Magnetic field		High-frequency electric field	
	0~100 K	100 K~200 K	0~100 K	100 K~200 K	200 K~10 M	10 M~2 G
ε393	6.0886	4.5349	2.6687	0.0540	8.2055	4.9254

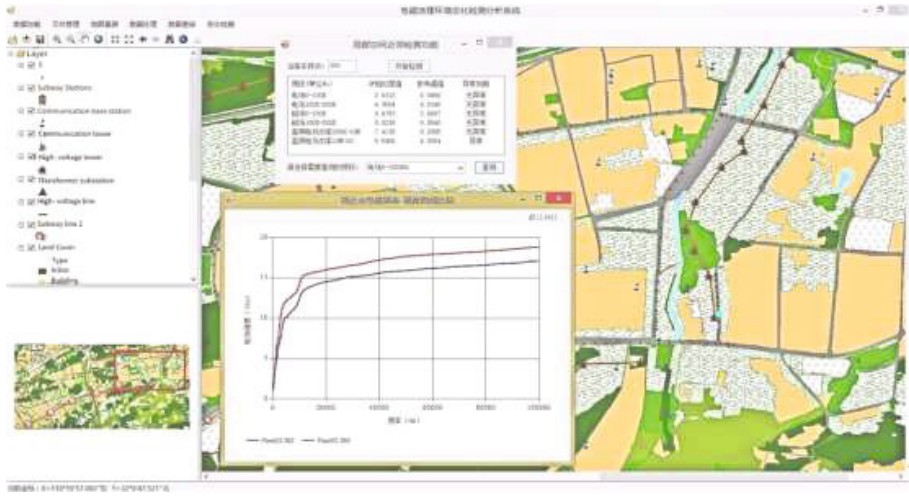

Figure 6: Local anomaly detection of ID 393.

place; otherwise, it is a normal point where the electromagnetic data changes within a normal range.

4.3. Global Detection for Anomalous Changes in Electromagnetic Geographic Environment. The local anomaly detection method can monitor the electromagnetic condition in real time, but it is hard to make overall analyses of the geographic environment. Therefore, a global detection method is proposed to find all anomalous points in the study area. The search process is similar to local detection, which should find adjacent points of all sampling points firstly and then calculate the curve similarity between each point and its neighboring points. The global detection method can figure out the frequency and location of all anomalous points.

To find all spatial adjacent points of each sampling point, multiple characteristics are first considered in this research, such as the vehicle trajectory, traffic rules (straight, left turn, right turn, etc.), and structure of road network (T intersection, crossroad, etc.). Based on that, we build the spatial index by the K-dimensional (KD) tree algorithm [31], which regards the positioning data (longitude and latitude) as two-dimensional data (x, y) and queries the neighboring points of each sampling point under different spatial distribution patterns. After establishing the KD tree index, adjacent points can be found quickly by setting the corresponding search radius. Moreover, it is also necessary to clarify the relevant anomaly threshold. As such, we adopt the randperm function in Matlab to change the numbering of all sampling points and select 150 points randomly. Afterwards, adjacent points of these random points are searched by the constructed KD tree index, and their similarities of the frequency-intensity curve at each frequency band are

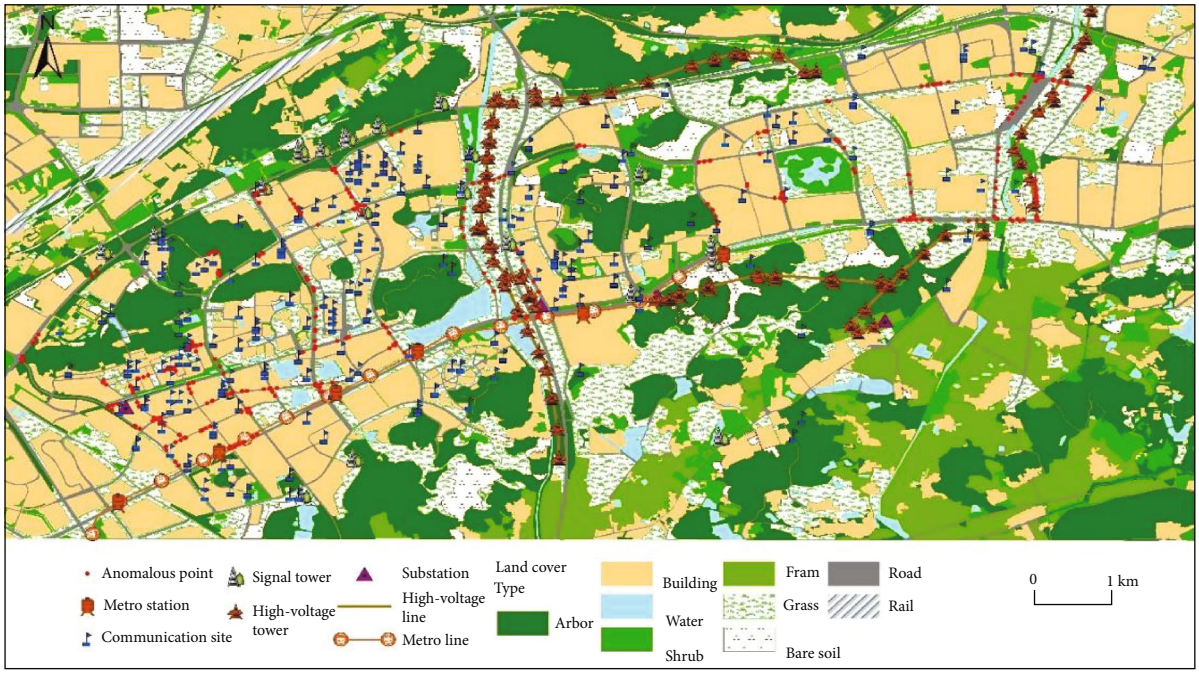

(a)

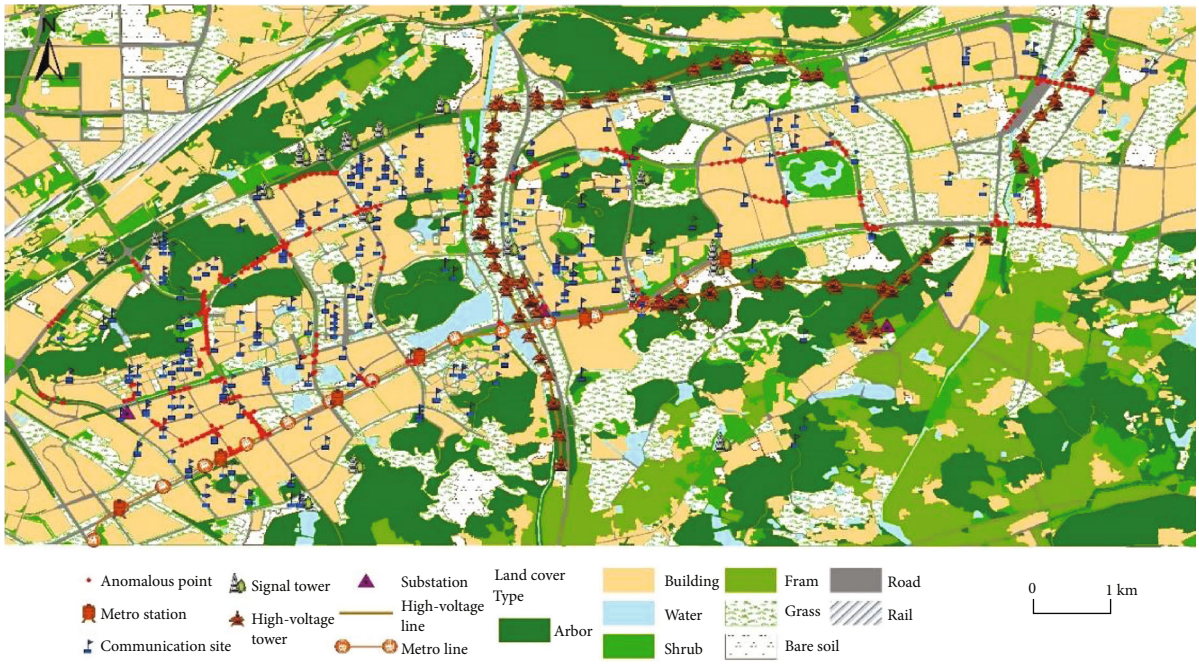

(b)

Figure 7: Continued.

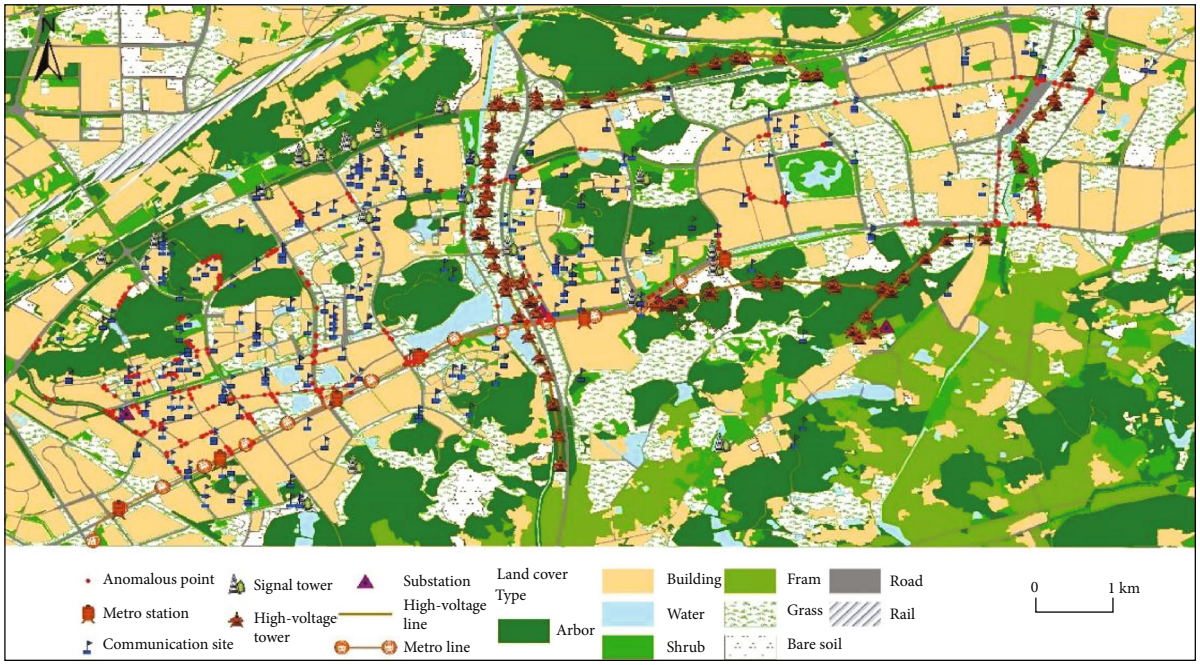

(c)

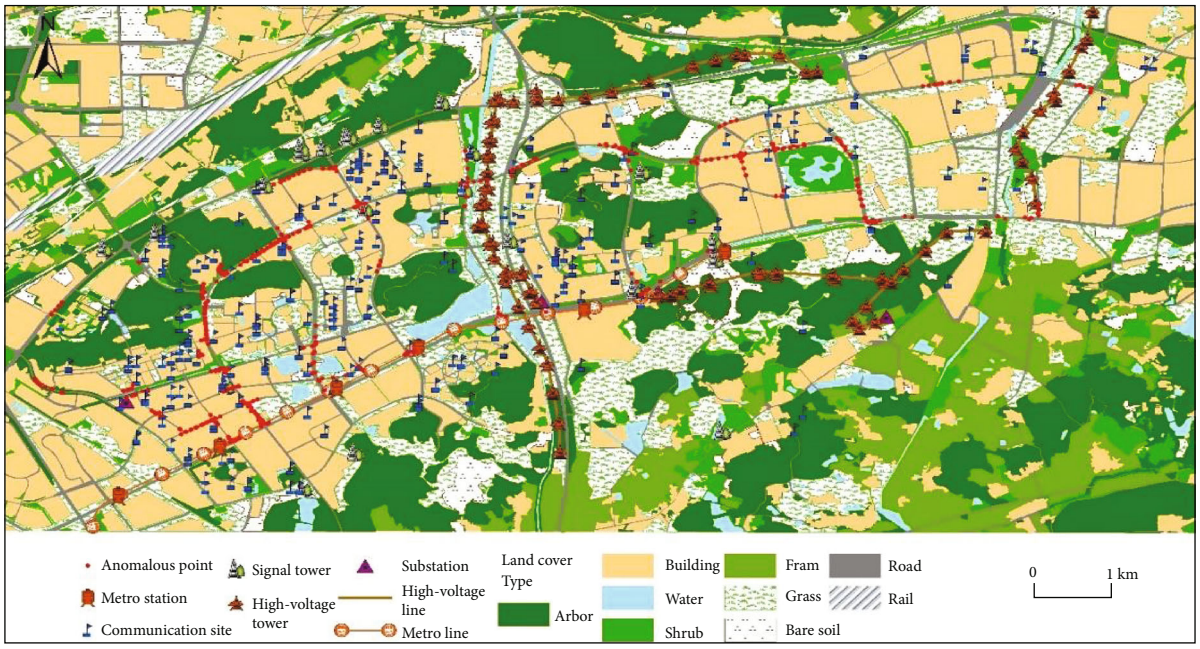

(d)

Figure 7: Continued.

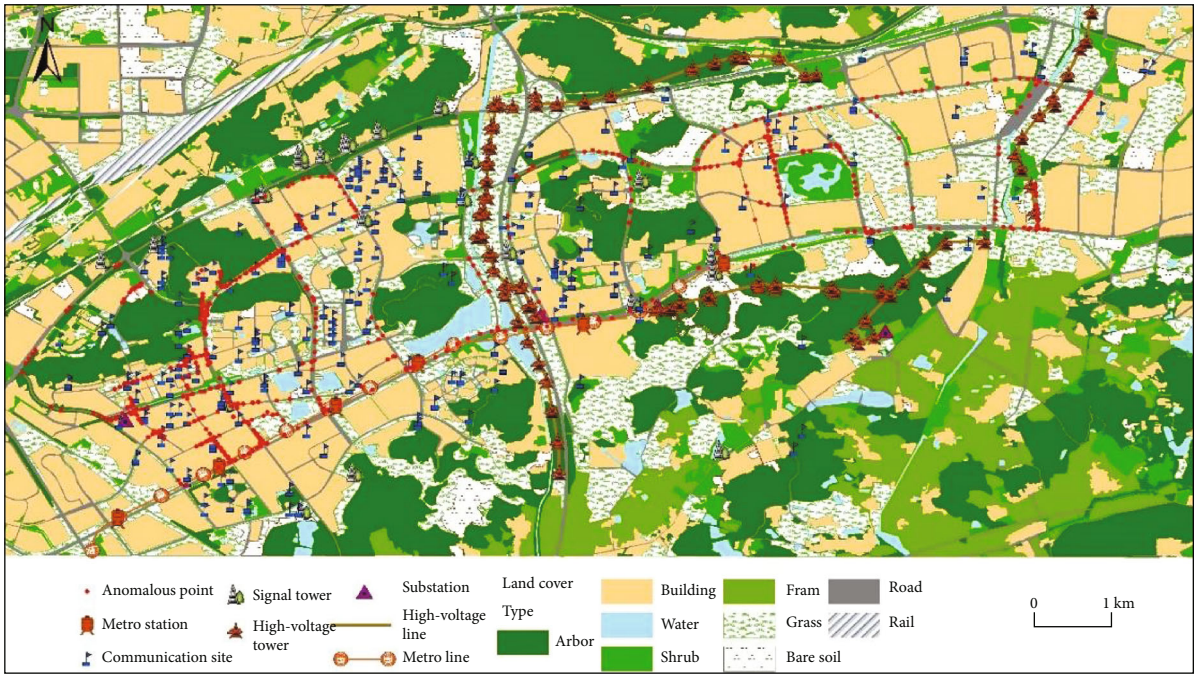

(e)

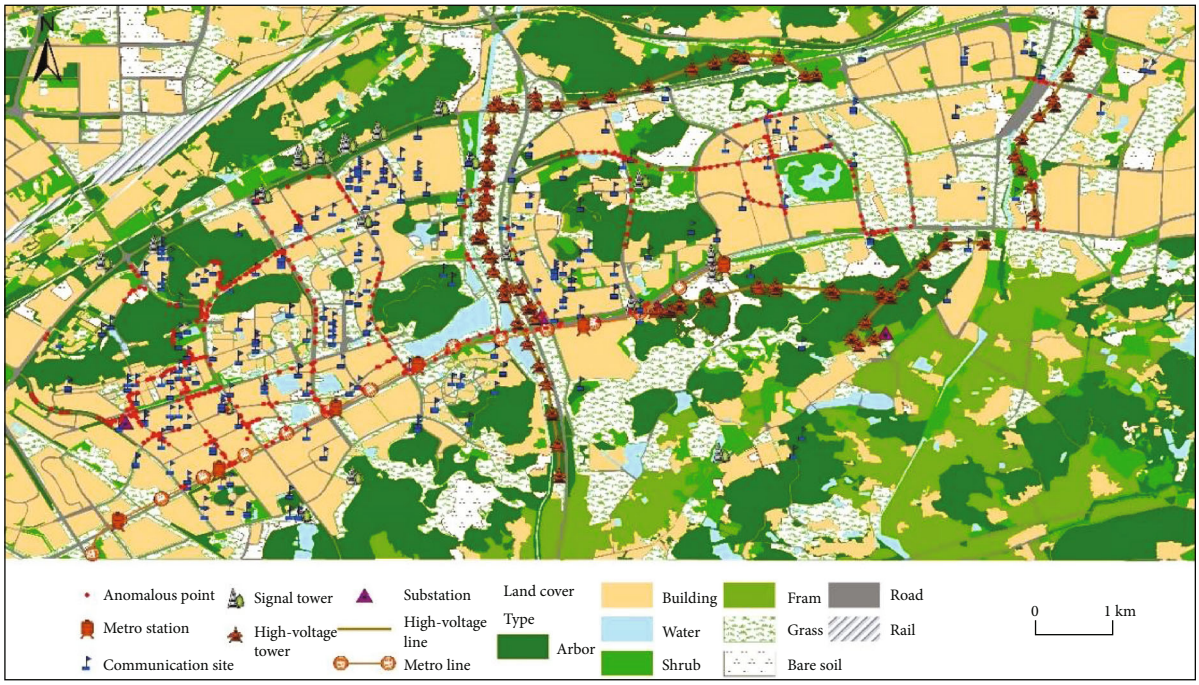

(f)

Figure 7: Spatial distribution pattern of anomalous points in each frequency: (a) electric field (0~100 K); (b) electric field (100 K~200 K); (c) magnetic field (0~100 K); (d) magnetic field (100 K~200 K); (e) high-frequency electric field (200 K~10 M); (f) high-frequency electric field (10 M~2 G).

calculated by discrete Fréchet distance. For each frequency band, we calculate the maximum curve similarity between each selected point and its adjacent points by

$$dF_i = \max\left\{\text{Dist}\left(a_i, b_j\right)\right\}, b_j \in B_i, \quad (10)$$

where a_i represents the sample points, B_i is the adjacent point set of this sample point, Dist () is a function used to calculate the discrete Fréchet distance, and dF_i is the largest value of curve similarity between each sample point and its adjacent points.

After the training and learning of the randomly selected points, we accumulate all dF_i and calculate their average

Table 5: Number of anomalous points in each frequency.

Frequency (Hz)	Electric field		Magnetic field		High-frequency electric field	
	0~100 K	100 K~200 K	0~100 K	100 K~200 K	200 K~10 M	10 M-2 G
Number of points	340	484	354	513	631	478

value as the thresholds $\varepsilon_{\max}$ for each frequency range. It can be expressed as Equation (11), and the results are listed in Table 2:

$$\varepsilon_{\max} = \frac{\sum_{i=1}^{N} dF_i}{N}, \tag{11}$$

where N represents the number of sampling points which are selected randomly.

5. Anomaly Detection and Analysis for Electromagnetic Environment

5.1. Local Anomaly Detection and Analysis. To realize the autoanomaly detection of electromagnetic environment, we integrate the above methods and develop a detecting system by C# language on Visual Studio 2010. This system adopts object-oriented technique and secondary development of GIS (Geographic Information System) and can provide various functions, such as data management, basic map operations, data processing, data query, and change detection. Among these, the change detection module supports the detection from both local and global perspectives. Taking the sampling point (ID 393) as an example, the discrete Fréchet distances between these points and its three adjacent sampling points are listed in Table 3.

Moreover, the threshold of ID 393 for anomaly detection is calculated by Equation (9) with these three neighboring points, which can be seen in Table 4.

For ID 393, we compare its similarity of frequency-intensity curves and ε393. The results show that when VEEMS approaches ID 393, the similarity exceeds the given threshold only at the frequency band of 10 M~20 G for the high-frequency electric field, which indicates that ID 393 has a relative drastic anomalous change at this band compared with its neighboring points. With the application of this method, VEEMS can find changing electromagnetic phenomena and detect the corresponding frequency band in time (Figure 6). Moreover, after the consideration of the surrounding environment, it is possible for users to speculate the cause of anomalous changes.

5.2. Global Anomaly Detection and Analysis. According to the global anomaly detection proposed above, we detect in the entire area and explore anomalous signals from all sampling points. To reduce errors generated by VEEMS, we repeat the experiment twice in a round trip and figure out the spatial distribution pattern of anomalous points (Figure 7), and the number of anomalous points is listed in Table 5.

According to Table 5, numbers of anomalous points are relatively small for the frequency of 0-100 kHz of both electric and magnetic fields, but larger in the middle-high frequencies. Moreover, most anomalous points are mainly distributed in densely built-up areas, which can be seen in Figure 7. It can be explained that since a large number of residents live in this area, more household appliances (e.g., hair dryers, microwave ovens, TVs, and refrigerators), electronic devices (e.g., mobile phones and computers), and broadcast communication base stations are used in their daily life. These devices can produce electromagnetic waves to interfere local environment and lead to anomalous changes. Additionally, the anomalous points also appear in arterial roads or intersections constantly. Due to the large traffic in these areas, electromagnetic waves radiated by vehicles may easily cause changes in the surrounding environment.

The anomalous points of different frequency bands are also different. For the frequencies of 0-100 kHz and 100 kHz-200 kHz, the number of anomalies in the magnetic field is larger than the same frequency in the electric field. However, their spatial distribution patterns are generally consistent (Figures 7(a)–7(d)). According to the classification standard of electromagnetic radiation frequency, only a few sources generate radiation within the frequency of 0 ~100 kHz, and most of these sources are not located in the daily residential area. Thus, points at this frequency are fewer and scattered in the research area. Furthermore, anomalous points within frequencies of 0-100 kHz, 100 kHz-200 kHz, and 10 MHz~2 GHz are not only distributed near buildings but also spread throughout public facilities, such as communication sites, high voltage transmission lines, and subway lines continuously. To be specific, radiation sources within the frequency of 100 kHz~200 kHz are some pervasive facilities like underground pipelines and wireless communication systems. However, more radiation sources are concentrated in the high-frequency range of 200 kHz~2 GHz (especially in 200 kHz~10 MHz for the most), such as subway trains (2 MHz~26 MHz), mobile communication base stations (150 MHz~1800 MHz), and high-voltage power systems (3 MHz~30 MHz). These basic public infrastructures can affect a large area, so various electromagnetic anomalous changes can be detected within this high frequency in the geographic environment.

6. Conclusions

Electromagnetic radiation fields have important impacts on human health. With the rapid development of modern electricity, media, and communication technology, most people live in the electromagnetic radiation environment of different frequencies and intensities. Therefore, monitoring and evaluating the electromagnetic environment are essential preconditions for further environmental protection and control. In order to detect the abnormalities and reveal hidden

sources of electromagnetic radiation, this research first developed a vehicle-mounted electromagnetic environment monitoring system to make up the shortcomings of traditional detection schemes. Such system can collect electromagnetic data of full frequency as well as the positioning data quickly and provide a reliable data source for subsequent anomalous detection of electromagnetic radiation.

After obtaining the above data, this paper integrates ideas from the concept of ground object spectrum and generates the electromagnetic frequency-intensity curve to reflect the variation of electromagnetic intensity of different frequencies in the study area. In addition, according to the characteristics of frequency-intensity curves of different frequencies, several preprocessing methods, such as accumulative curve and digital filtering, are used to improve the authenticity and stability of data.

To analyze the constructed electromagnetic frequency-intensity curve, a similarity measurement based on discrete Fréchet distance is proposed to measure the curve similarity of spatial adjacent sampling points. The results are used to detect anomalous changes in the electromagnetic geographic environment from both local and global perspectives. On this basis, various research methods (e.g., object-oriented and GIS secondary development) are integrated to develop an anomaly detection and analysis system. This system has many functional modules, such as data preprocessing, data management and maintenance, attribute query, basic map operations, and electromagnetic change detection. Therefore, it can effectively diagnose and analyze anomalous changes of electromagnetic radiation of full frequencies in different geographical environments.

To sum up, this study is significant to master the conditions of electromagnetic environment, which regards the electromagnetic environment as an important geographic feature. It can enrich the connotation of traditional virtual geographic environment and improve the scientific management level of electromagnetic geographic environment. Although this research has made certain achievements, several areas still need to be explored in the future. First, the electromagnetic frequency-intensity curve constructed in this study expresses a relatively wide frequency range; it can speculate the type of radiation source according to the classification standard of electromagnetic radiation frequency and its surrounding environment, but hard to identify the exact source and location which leads to such anomalous changes. To fill this gap, further researches can refine the frequency range by considering frequencies of some important radiation sources. Additionally, electromagnetic radiation sources are growing rapidly, while different sources may have different propagation and attenuation laws of electromagnetic radiation. Based on these laws, subsequent researches can conduct physical inversion to verify the speculative location of anomalous radiation sources, which is significant to improve the detection accuracy.

Data Availability

Both electric and magnetic field data after preprocessing can be downloaded at the following link: https://pan.baidu.com/s/12DRBIOeptZsqYCQpSInmsA, with the password wf2v.

Conflicts of Interest

The authors declare that there is no conflict of interest regarding the publication of this paper.

Acknowledgments

This research was funded by the Key Fund of National Natural Science Foundation of China, grant number 41631175; the National Key Research and Development Program of China, grant number 2017YFB0503500; and the Open Foundation of Smart Health Big Data Analysis and Location Services Engineering Lab of Jiangsu Province, grant number SHEL221 002.

References

[1] C. Constable, "Earth's electromagnetic environment," *Surveys in Geophysics*, vol. 37, no. 1, pp. 27–45, 2016.

[2] M. Füllekrug and A. C. Fraser-Smith, "The earth's electromagnetic environment," *Geophysical Research Letters*, vol. 38, no. 21, pp. 3–7, 2011.

[3] J. D. Kraus, *Electromagnetics with Applications (Fifth Edition)*, International Thomson Business Press, Boston, 1999.

[4] M. Y. Wang, Y. H. Sheng, Y. Y. Huang et al., "Spatial interpolation method of electromagnetic geographical environment monitoring data," *Journal of Geo-information Science*, vol. 19, pp. 872–879, 2017.

[5] A. K. Dhami, "Study of electromagnetic radiation pollution in an Indian city," *Environmental Monitoring and Assessment*, vol. 184, no. 11, pp. 6507–6512, 2012.

[6] A. Lerchl, "Electromagnetic pollution: another risk factor for infertility, or a red herring?," *Asian Journal of Andrology*, vol. 15, no. 2, pp. 201–203, 2013.

[7] S. A. Pappert, S. C. Lin, R. J. Orazi, M. N. McLandrich, P. K. L. Yu, and S. T. Li, "Broadband electromagnetic environment monitoring using semiconductor electroabsorption modulators," in *Proceedings of SPIE the International Society for Optical Engineering*, vol. 1476, Orlando, FL, USA, 1991.

[8] L. Ioriatti, M. Martinelli, F. Viani, M. Benedetti, and A. Massa, "Real-time distributed monitoring of electromagnetic pollution in urban environments," *International Geoscience and Remote Sensing Symposium*, vol. 5, pp. 100–103, 2009.

[9] E. Vance, W. Graf, and J. Nanevicz, "Unification of electromagnetic specifications and standards," *Part I- Evaluation of Existing Practices*, 1980.

[10] Ö. Genç, M. Bayrak, and E. Yaldiz, "Analysis of the effects of GSM bands to the electromagnetic pollution in the RF spectrum," *Progress In Electromagnetics Research*, vol. 101, pp. 17–32, 2010.

[11] S. S. Durduran, O. Uygunol, and L. Seyfi, "Mapping of electromagnetic pollution at 1800 MHz GSM (global system for mobile communication) frequency in Konya," *Scientific Research and Essays*, vol. 5, no. 18, pp. 2664–2672, 2010.

[12] P. García-Díaz, S. Salcedo-Sanz, J. A. Portilla-Figueras, and S. Jiménez-Fernández, "Mobile network deployment under electromagnetic pollution control criterion: an evolutionary algorithm approach," *Expert Systems with Applications*, vol. 40, no. 1, pp. 365–376, 2013.

[13] L. Rossetto, P. Tenti, and A. Zuccato, "Electromagnetic compatibility issues in industrial equipment," *IEEE Industry Applications Magazine*, vol. 5, no. 6, pp. 34–46, 1999.

[14] N. Djuric, M. Prsa, V. Bajovic, and K. Kasas-Lazetic, "Serbian remote monitoring system for electromagnetic environmental pollution," in *2011 10th International Conference on Telecommunication in Modern Satellite Cable and Broadcasting Services (TELSIKS)*, pp. 701–704, Nis, Serbia, October 2011.

[15] O. Postolache, P. Girão, S. Antunes, and F. Tavares, "Global instrumentation network for broadband RF spectrum monitoring," *Proceedings of Conference on Telecommunications*, vol. 1, pp. 1–4, 2009.

[16] J. A. Stine and D. L. Portigal, *Spectrum 101: An Introduction to Spectrum Management*, Mitre Technical Report, McLean, Virginia, 2004.

[17] L. Guenda, E. Santana, A. Collado, K. Niotaki, N. B. Carvalho, and A. Georgiadis, "Electromagnetic energy harvesting—global information database," *Transactions on Emerging Telecommunications Technologies*, vol. 25, no. 1, pp. 56–63, 2014.

[18] J. Lefman, R. Morrison, and S. Subramaniam, "Automated 100-position specimen loader and image acquisition system for transmission electron microscopy," *Journal of Structural Biology*, vol. 158, no. 3, pp. 318–326, 2007.

[19] I. Lingvay, A. Voina, C. Lingvay, and C. Mateescu, "The impact of the electromagnetic pollution of the environment on the complex build-up media," *Revue Roumaine des Sciences Techniques - Serie Électrotechnique et Énergétique*, vol. 53, pp. 95–111, 2008.

[20] H. Yagou, Y. Ohtake, and A. Belyaev, "Mesh smoothing via mean and median filtering applied to face normal," in *Geometric Modeling and Processing. Theory and Applications. GMP 2002. Proceedings*, pp. 124–131, Wako, Japan, 2002.

[21] K. Ito, "Gaussian filter for nonlinear filtering problems," in *Proceedings of the 39th IEEE Conference on Decision and Control (Cat. No.00CH37187)*, vol. 45no. 5, pp. 1218–1223, Sydney, NSW, Australia, 2000.

[22] T. W. Beck, J. M. Defreitas, J. T. Cramer, and J. R. Stout, "A comparison of adaptive and notch filtering for removing electromagnetic noise from monopolar surface electromyographic signals," *Physiological Measurement*, vol. 30, no. 4, pp. 353–361, 2009.

[23] L. Sheng, W. Bangmin, and Z. Lanyong, "Intelligent adaptive filtering algorithm for electromagnetic-radiation field testing," *IEEE Transactions on Electromagnetic Compatibility*, vol. 59, no. 6, pp. 1765–1780, 2017.

[24] S. E. Stein and D. R. Scott, "Optimization and testing of mass spectral library search algorithms for compound identification," *Journal of the American Society for Mass Spectrometry*, vol. 5, no. 9, pp. 859–866, 1994.

[25] M. P. Dubuisson and A. K. Jain, "A modified Hausdorff distance for object matching," in *Proceedings of 12th International Conference on Pattern Recognition*, vol. 1, pp. 566–568, Jerusalem, Israel, 1994.

[26] S. Shao, H. Liu, L. Xiao, and H. Wang, "A complex linear feature of Fréchet distance matching method," *Geomatics and Information Science of Wuhan University*, vol. 43, no. 4, pp. 516–521, 2018.

[27] H. Alt and M. Godau, "Computing the Fréchet distance between two polygonal curves," *International Journal of Computational Geometry & Applications*, vol. 5, pp. 75–91, 1995.

[28] F. Barbaresco, "Geometric radar processing based on Fréchet distance: information geometry versus optimal transport theory," in *Proceedings of the 2011 12th International Radar Symposium (IRS)*, pp. 663–668, Leipzig, Germany, September 2011.

[29] Y. Zhou, F. Qiu, A. A. Al-Dosari, and M. S. Alfarhan, "ICESat waveform-based land-cover classification using a curve matching approach," *International Journal of Remote Sensing*, vol. 36, no. 1, pp. 36–60, 2015.

[30] T. Eiter and H. Mannila, *Computing discrete Fréchet distance*, Technical Report CD-TR 94/64, Christian Doppler Laboratory for Expert Systems, TU Vienna, Austria, 1994.

[31] J. L. Bentley, "Multidimensional binary search trees used for associative searching," *Communications of the ACM*, vol. 18, no. 9, pp. 509–517, 1975.